A MODIFIED ACTIVE DISTURBANCE REJECTION CONTROL APPLIED TO THE TWIN-ROTOR SYSTEM WITH OUTPUT QUANTIZATION

J. A. Dulce-Galindo*, Leonardo A. B. Tôrres†, Guilherme Vianna Raffo†

*Graduate Program in Electrical Engineering – PPGEE
Federal University of Minas Gerais – UFMG
Av. Antônio Carlos 6627, 31270-901, Belo Horizonte, MG, Brazil

†Department of Electronic Engineering – DELT
Federal University of Minas Gerais – UFMG
Av. Antônio Carlos 6627, 31270-901, Belo Horizonte, MG, Brazil

jaimearturodg@ufmg.br, leotorres@ufmg.br, raffo@ufmg.br

Abstract— The model-free strategy called Active Disturbance Rejection Control (ADRC) is applied to the pitch attitude control of a Twin-Rotor system. The original ADRC strategy is modified to account for the quantization of system's pitch angle associated with the use of an incremental encoder. The modifications include the use of Algebraic Differentiator to smooth out the measured pitch angle, together with a Robust and Exact Differentiator (RED) to estimate the main rotor propeller angular speed. Experimental results are provided to illustrate the effectiveness of the modified ADRC strategy.

Keywords— ADRC, quantization error, differentiation, Twin-rotor.

Resumo— A estratégia de controle não baseada em modelagem matemática do sistema, chamada de Controle por Rejeição Ativa de Perturbação (ADRC), é aplicada ao controle do ângulo de arfagem de um sistema Rotor-Duplo. A estratégia original do ADRC é modificada para que seja possível considerar a quantização das medidas de ângulo de arfagem associada ao uso de um *encoder* incremental. As modificações incluem o uso de um Diferenciador Algébrico para se obter um sinal suavizado correspondente ao ângulo de arfagem medido, juntamente com um Diferenciador Exato e Robusto para se obter uma estimativa da velocidade de rotação do rotor principal. Resultados experimentais são fornecidos para ilustrar a eficácia da estratégia ADRC modificada.

Palavras-chave— ADRC, erro de quantização, diferenciação, Rotor-duplo.

1 Introduction

The design of controllers for nonlinear dynamical systems usually relies on specific strategies for specific classes of systems, with these classes defined by properties associated with the underlying mathematical models of the systems under consideration (Slotine and Li, 1990; Khalil, 2001).

Contrary to this well-established approach of investigating the control problem in rigorous mathematical grounds based on well-defined mathematical models, recently there has been some very interesting papers defending the opposite idea of using "model-free" strategies to control nonlinear systems. Particularly, one can highlight the influential work by the professor[1] Han (2009), where a new "universal" control strategy, called the Active Disturbance Rejection Control (ADRC) method, is purposely designed as a replacement for the popular PID controller. In the same vein, Fliess and Join (2013) have presented the idea of using time-derivatives estimation as a step to control nonlinear systems without knowing the underlying mathematical model.

The common point between these two model-free strategies can be seen as the attempt to cancel the original dynamics of the system by means of an appropriate estimation of high-order time-derivatives of the system's output. This means that the presence of abrupt changes in the output signal, as it would be expected if the system's output is quantized, could be deleterious to the performance of the closed-loop system.

Following the idea of incrementally modifying the original ADRC strategy to handle specific problems, e.g. as presented in (Zheng and Gao, 2016), in this work a modified ADRC strategy is proposed with two main objectives, namely: *(i)* to present to a larger Brazilian control community the ADRC strategy (Han, 2009), together with some very interesting concepts related to the work in (Fliess and Join, 2013); and *(ii)* to achieve improved results using the ADRC method, even when there is quantization in the output signal. The improvement depends crucially on the ideas in (Fliess and Join, 2013) to smooth the quantized output signal. To show the effectiveness of the proposed strategy, experimental results on the pitch attitude control for a Twin Rotor System (TRS) (Feedback, 2006) is provided.

2 Model-Free Control Techniques

To illustrate the main general ideas in the model-free control techniques presented in (Han, 2009) and (Fliess and Join, 2013), consider a Single-Input Single-Output (SISO) input affine nonlinear dynamical system with well-defined relative

[1]Deceased in April, 2008. See the message from the Editor-in-Chief in (Han, 2009).

degree r. It is worth noticing that this class encompasses a large set of dynamical systems. In this case, one can represent the system using a special set of coordinates such that part of the state vector is comprised by the output and its corresponding time-derivatives (Isidori, 1989), i.e.

$$\begin{aligned} y^{(r)} =& F(y, \dot{y}, \dots, y^{(r-1)}, z) \\ &+ G(y, \dot{y}, \dots, y^{(r-1)}, z)u, \\ \dot{z} =& W(y, \dot{y}, \dots, y^{(r-1)}, z), \end{aligned} \tag{1}$$

where is the output; $\dot{y}, \dots, y^{(r-1)}$ are its successive time-derivatives up to order $r-1$; $z \in \mathbb{R}^{n_{\text{id}}}$ is the vector of state variables associated with the system's internal dynamics; $u \in \mathbb{R}$ is the input; and $F(\cdot) : \mathbb{R}^{r+n_{\text{id}}} \to \mathbb{R}$, $G(\cdot) : \mathbb{R}^{r+n_{\text{id}}} \to \mathbb{R}$, and $W(\cdot) : \mathbb{R}^{r+n_{\text{id}}} \to \mathbb{R}^{n_{\text{id}}}$ are bounded nonlinear functions, with $G(\cdot)$ nonzero in an open set. By adding an even stronger requirement that the system's internal dynamics are input-to-state stable (Khalil, 2001) with respect to $y, \dot{y}, \dots, y^{(r-1)}$, or that there is no internal dynamics whatsoever (i.e. the system has full relative degree), a simplified version of (1) can be considered:

$$y^{(r)} = F(t) + G(t)u, \tag{2}$$

with $F(t) \equiv F(y, \dot{y}, \dots, y^{(r-1)}, z)$ and $G(t) \equiv G(y, \dot{y}, \dots, y^{(r-1)}, z)$ bounded functions. In both strategies (Han, 2009; Fliess and Join, 2013) the authors propose the use of a feedback linearizing like control law

$$u = \frac{1}{\hat{G}_{\text{c}}} \left(-\hat{F}(t) + v \right), \tag{3}$$

with $\hat{F}(t) : \mathbb{R} \to \mathbb{R}$ an estimative of the function $F(t)$; $\hat{G}_{\text{c}} \in \mathbb{R}$ a nonzero constant used as an approximation for $G(t)$; and v a virtual control input whose final form will make (2) resemble, in both cases, a stable differential equation on the error variable $e(t) = y_{\text{ref}}(t) - y(t)$, where $y_{\text{ref}}(t)$ is the reference signal to be tracked (Han, 2009; Fliess and Join, 2013).

One key difference between these strategies is the way the approximation $\hat{F}(t)$ is obtained. However, in both cases the process of computing $\hat{F}(t)$, and therefore the energy of the control input in (3), depends on the smoothness of the system's output signal, as it will be illustrated in the next sections.

2.1 ADRC Fundamentals

A key subsystem in the ADRC structure (Han, 2009), shown in Figure 1, is the so-called *Extended State Observer* (ESO), which is used to provide an estimative of $F(t)$ in (2). Consider the augmented system

$$\begin{aligned} \dot{x}_1 &= x_2,\ \dot{x}_2 = x_3,\ \cdots, \\ \dot{x}_r &= x_{r+1} + G(t)u, \\ \dot{x}_{r+1} &= D(t),\ \ y = x_1, \end{aligned}$$

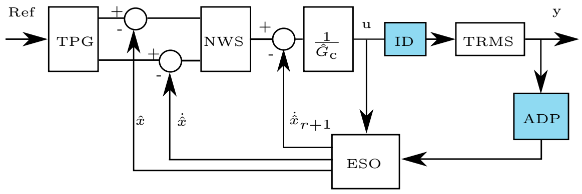

Figure 1: Modified ADRC topology. Subsystems ID and ADP are novel additions.

which is equivalent to (2) as long as $x_{r+1} = F(t)$, such that $D(t) \equiv \frac{dF(t)}{dt}$. From this description, a Luemberger-like observer can be designed as

$$\begin{aligned} \dot{\hat{x}}_1 &= \hat{x}_2 + \ell_1(y - \hat{x}_1), \\ \dot{\hat{x}}_2 &= \hat{x}_3 + \ell_2(y - \hat{x}_1),\ \cdots, \\ \dot{\hat{x}}_r &= \hat{x}_{r+1} + \hat{G}_{\text{c}}u + \ell_r(y - \hat{x}_1), \\ \dot{\hat{x}}_{r+1} &= \ell_{r+1}(y - \hat{x}_1), \end{aligned} \tag{4}$$

where $\ell_i(\cdot)$; $i = 1, 2, \dots, r+1$; are scalar, not necessarily linear, functions of the observation error $y - \hat{x}_1$. Clearly, the structure in (4) can be seen as a Unknown Input Observer (UIO) (Takahashi and Peres, 1999) with $D(t)$ and $(G(t) - \hat{G}_{\text{c}})u(t)$ as unknown inputs, such that the observer state $\hat{x}_{r+1}$ is used as an estimative for $F(t)$ in (2); i.e. $\hat{F}(t) = \hat{x}_{r+1}$ in (3).

Other two subsystems necessary to implement the ADRC strategy are the *Transient Profile Generator* (TPG), and the *Nonlinear Weighted Sum* (NWS) (see Fig. 2 in Han (2009)).

The TPG is a second-order dynamical system described by

$$\dot{\xi}_1 = \xi_2,\ \dot{\xi}_2 = -p\,\text{sign}\left(\xi_1 - y_{\text{ref}} + \frac{\xi_2|\xi_2|}{2p} \right), \tag{5}$$

with $y^{\text{s}}_{\text{ref}}(t) = \xi_1$, and p a smoothing parameter. System (5) acts similarly to a low-pass filter by receiving the reference signal $y_{\text{ref}}(t)$ as its input and producing a continuously differentiable output $y^{\text{s}}_{\text{ref}}(t)$, that otherwise follows closely the original reference signal. In addition, note that the accompanying signal $\dot{y}^{\text{s}}_{\text{ref}}(t) = \xi_2$ is also made available for control purposes.

Finally, in the NWS subsystem the virtual control v in (3) is computed as a possibly nonlinear combination of $e_1 = y^{\text{s}}_{\text{ref}}(t) - \hat{x}_1$, and $e_2 = \dot{y}^{\text{s}}_{\text{ref}}(t) - \hat{x}_2$. Particularly, in this paper, we have the linear combination

$$v = K_{\text{p}}e_1 + K_{\text{d}}e_2, \tag{6}$$

with $K_{\text{p}}, K_{\text{d}} \in \mathbb{R}$ tuning parameters.

2.2 Differentiation Strategies

In Fliess and Join (2013) an alternative approach to the ESO is employed to compute $\hat{F}(t)$ in (3) by directly differentiating the system's output $y(t)$; i.e. from (2) one has that $\hat{F}(t) \approx y^{(r)} - \hat{G}_{\text{c}}u(t)$, assuming that $u(t)$ is known. To differentiate $y(t)$, the main idea is to consider that, for the last T seconds, the system's output can be approximated by a polynomial time function with a prescribed degree of nonlinearity m, such that

$$y(\tau) \approx a_0 + a_1\tau + \ldots + a_m\tau^m,\ \ \tau \in [t-T, t], \quad (7)$$

where the coefficients a_i, $i = 0, 1, 2, \ldots, m$, are computed based on the measured values of $y(t)$ in the last time window. Their computation is derived following the rules of the so-called Operational Calculus in the Laplace variable s, as detailed in Zehetner et al. (2007) and Mboup et al. (2009). Interestingly, the coefficients computation depends only on time integrals, which makes them somewhat robust to noise, but introduces unavoidable time-delay in their estimation. Clearly, from the knowledge of the coefficients a_i, it is easy to estimate the time-derivatives of $y(t)$. This procedure will be called hereafter *Algebraic Differentiation Procedure* (ADP). Note that the ADP depends on the choice of the two parameters T and m, but it is implemented as a linear finite impulse response (FIR) digital filter, and therefore it is stable.

An alternative approach to compute time-derivatives is to consider the associated tracking control problem where a controller is designed to achieve $\lim_{t\to\infty}[x(t) - y(t)] = 0$, with $x(t)$ the state of the first-order pure integrator given by $\dot{x} = u$, and $x, u \in \mathbb{R}$. In this case, assuming the fulfillment of the zero error objective, the controller output signal $u(t)$ can be used as a estimative for the time derivative of the signal $y(t)$. Following this approach, in the so-called *Robust and Exact Differentiator* (RED) (Levant, 1998), a second-order sliding mode controller (Shtessel et al., 2014, Chapter 4) is employed to guarantee finite-time convergence of the error, such that a time derivative estimation with good accuracy becomes available in short time. Despite this, the presence of high frequency additive noise can degrade considerably the performance of the RED.

In this work both differentiation strategies ADP and RED will be employed, respectively, to counteract the output signal quantization, and to provide an estimative of one of the system's state variables not directly measured (Section 4).

3 Twin-Rotor Description

The Twin-Rotor System, shown in Figure 2, is a two-degrees of freedom electromechanical system used in didactic control experiments (Feedback, 2006).

By locking up the yaw movement around the vertical axis, the rod that unites the two propellers is allowed to swing up and down as it changes the pitch angle orientation around the horizontal axis, and the TRS becomes a one-degree of freedom mechanism.

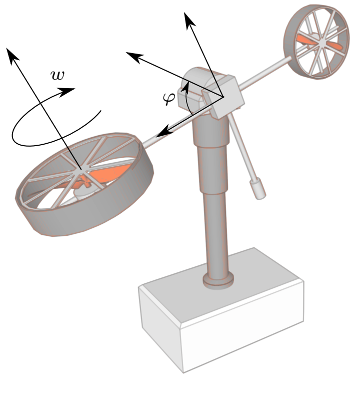

Figure 2: Twin-Rotor System – TRS.

The main propulsive torque used to control the pitch angle is associated with the rotational speed ω shown in Figure 2, which depends on the input voltage applied to a DC motor that drives the propeller. The pitch angle is measured by means of an incremental encoder with limited resolution, leading to quantization of system's output.

By applying Newton's second law to the rotational movement around the horizontal axis, and by representing the DC motor dynamics as a first order linear system; i.e. by neglecting the DC motor armature electrical current dynamics; one has that (Feedback, 2006)

$$\begin{aligned} \dot{x}_1 &= x_2, && (8)\\ I_\mathrm{h}\dot{x}_2 &= T_\mathrm{p}(x_3) - T_\mathrm{w}(x_1) - T_\mathrm{f}(x_2), && (9)\\ \tau_\mathrm{m}\dot{x}_3 &= -b_\mathrm{m}x_3 + k_\mathrm{m}u, && (10)\end{aligned}$$

where $x_1 = \varphi$ is the pitch angle; $x_2 = \dot{\varphi}$ is the angular speed around the horizontal axis; $x_3 = \omega$ (see Figure 2) is the rotational speed of the main propeller; u is the DC motor input voltage; with I_h the Twin-Rotor moment of inertia around the horizontal axis; τ_m, b_m and k_m are the mechanical time constant, viscous friction coefficient and steady-state gain, respectively, of the DC motor that drives the propeller. The net mechanical torque applied to the system is the sum of three contributions, namely the propulsive torque

$$T_\mathrm{p}(x_3) = \alpha_1 x_3^2 + \alpha_2 x_3; \quad (11)$$

with $\alpha_1 > 0$, $\alpha_2 > 0$ propeller thrust coefficients; the weight force restoration torque (the center of gravity does not coincide with the center of rotation) $T_\mathrm{w}(x_1) = m_\mathrm{g}\sin(x_1)$; with $m_\mathrm{g} > 0$ a parameter equal to the product of the weight force times the distance from the center of mass to the horizontal axis; and the viscous friction torque $T_\mathrm{f}(x_2) = b_\mathrm{f}x_2$; with $b_\mathrm{f} > 0$ the friction coefficient.

The TRS parameters $m_\mathrm{g} = 0.3199\,\mathrm{Nm}$, $I_\mathrm{h} = 7.02\times10^{-2}\,\mathrm{kg\,m^2}$, $\alpha_1 = 0.0152\,\mathrm{Nm/(rad/s)^2}$, $\alpha_2 = 0.0738\,\mathrm{Nm/(rad/s)}$, $b_\mathrm{f} = 11.5\times10^{-3}\,\mathrm{Nms/rad}$, $\tau_\mathrm{m} = 0.7980\,\mathrm{s}$, $k_\mathrm{m} = 1.2178\,\mathrm{(rad/s)/V}$ and $b_\mathrm{m} = 1.1106$ were estimated from open-loop input-output data collected in seven different experiments. By minimizing the mean squared error between the measured pitch angle and the simulated output for the same input voltage signal, the optimal set of parameters was searched for, taking as initial values the nominal parameters in (Feedback, 2006).

4 A Modified ADRC

Quantization of the system's output signal introduces high frequency content associated with abrupt changes in the measured values. In the case of the Twin-Rotor, this is a consequence of using an incremental encoder to measure the pitch angle. In this work a smoothing technique based on the use of an *Algebraic Differentiation Procedure* (ADP) (see Section 2.2) is employed to provide a differentiable approximation of the system's output to the ESO input (see Figure 1). This modification results in lower energy for the control signal variation, as it will be shown in Section 5.

In addition, an *Inverse Dynamics* (ID) subsystem is used to drive indirectly the Twin-Rotor propulsive torque. This is accomplished by computing the necessary input voltage to be applied to the TRS main rotor in order to achieve a target rotational speed associated with a desired propulsive torque as computed by the ADRC strategy. More specifically, from (11), by assuming that $T_{\text{p}}(x_3) = T_{\text{p}}^{\text{d}}(t)$, at each time instant, the positive value $x_3^{\text{d}}(t)$ that satisfies the polynomial equation $T_{\text{p}}^{\text{d}}(t) = \alpha_1 (x_3^{\text{d}}(t))^2 + \alpha_2 x_3^{\text{d}}(t)$ is determined. The input voltage is then computed, from (10), as

$$u(t) = \frac{1}{k_{\text{m}}} \left[\tau_{\text{m}} \mu(t) + b_{\text{m}} x_3^{\text{d}}(t) \right], \qquad (12)$$

where $\mu(t)$ is the output of a RED (Section 2.2) whose input is $x_3^{\text{d}}(t)$. Therefore, ideally the series connection of the blocks ID and TRS in Figure 1 would compose an equivalent second-order mechanical system whose input is torque, and whose output is pitch angle. It is worth noting that, although the approximated dynamical cancellation in (12) is not robust to parametric uncertainties in the DC motor parameters, by relying on the ADRC strategy, one expects to still have good results, as it was indeed the case as presented in Section 5.

5 Experimental Results

The modified ADRC performance is tested through five experimental results obtained in a real Twin-Rotor system. The experiments have been set to take 60s with sampling time 10ms, $m = 1$ and $T = 0.2$s for ADP in (7).

Initially, a first comparison analysis is performed between two control strategies based on pure ADRCs (see Section 2.1), in which one strategy, namely ADRC(3), makes use of an ESO for estimating three states while the other one, namely ADRC(4), estimates four states. In a first set of experiments these controllers are required to track a step reference signal, as shown in Figure 3, and in a second experiment these controllers are evaluated while tracking a sinusoidal reference signal, illustrated in Figure 4. The ADRC(3) was synthesized with the control gains $K_{\text{p}} = 4.5$ and $K_{\text{d}} = 1.5$, and functions $\ell_1(y - \hat{x}_1) = L_1(y - \hat{x}_1)$, $\ell_2(y - \hat{x}_1) = L_2 f(y - \hat{x}_1, 0.5, \delta)$, $\ell_3(y - \hat{x}_1) = L_3 f(y - \hat{x}_1, 0.25, \delta)$, in (4); with observer gains $L_1 = 28.8881$, $L_2 = 278.0063$ and $L_3 = 891.8834$, and $\delta = 1$, where (Han, 2009):

$$f(e, \alpha, \delta) = \begin{cases} e/\delta^{1-\alpha}, & |e| \leq \delta; \\ |e|^{\alpha} \text{sign}(e), & |e| > \delta. \end{cases}$$

Besides, the ADRC(4) was tuned with $K_{\text{p}} = 8$ and $K_{\text{d}} = 1.5$, and functions $\ell_1(y - \hat{x}_1) = L_1(y - \hat{x}_1)$, $\ell_2(y - \hat{x}_1) = L_2 f(y - \hat{x}_1, 0.5, \delta)$, $\ell_3(y - \hat{x}_1) = L_3 f(y - \hat{x}_1, 0.25, \delta)$, $\ell_4(y - \hat{x}_1) = L_4 f(y - \hat{x}_1, 0.25, \delta)$, in (4); with observer gains $L_1 = 36.7$, $L_2 = 505.3$, $L_3 = 3093.4$ and $L_4 = 7103.1$, and $\delta = 1$.

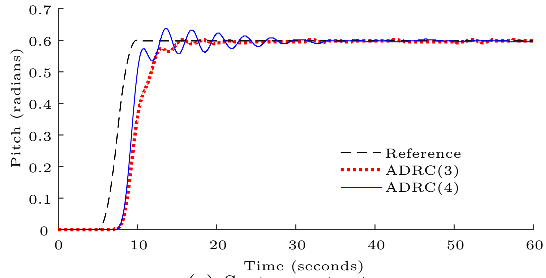

(a) System outputs.

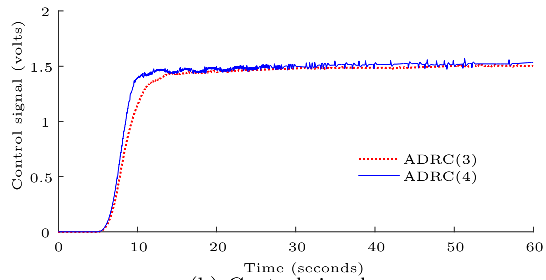

(b) Control signals.

Figure 3: Step response with ADRC techniques.

From Figure 3, one can observe that both pure ADRCs converge to the desired step reference, although both strategies presented time-delay due to the observer dynamics. Moreover, since the ADRC(4) was tuned to be more aggressive, its time response presented faster raising time, but at the cost of higher control effort and more oscillatory transient than ADRC(3).

In order to evaluate the pure ADRCs with time-varying reference signals and the same controllers and observer gains used previously, experiments with sinusoidal reference were obtained. From Figure 4, it is observed that neither ADRC(3) nor ADRC(4) were able to track the reference, destabilizing the TRS.

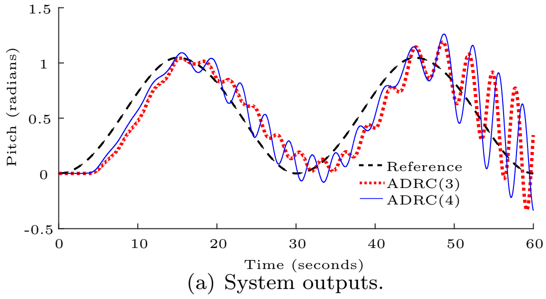

(a) System outputs.

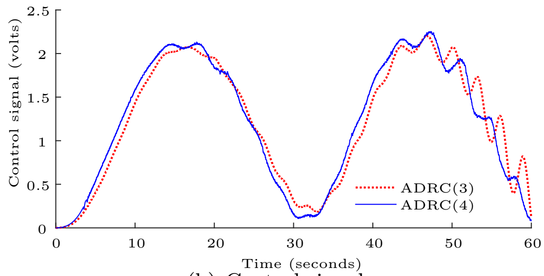

(b) Control signals.

Figure 4: Sinusoidal response with ADRC techniques.

On the other hand, to analyze the modifications proposed in this work, two set of experiments have been performed for comparing the modified ADRC ID (ADRC(3) with the ID block that uses the RED approach) against the modified ADRC ID ADP (ADRC(3) with the ID block that uses the RED approach, and with the ADP block). Again, results with step and sinusoidal reference signals were obtained for the third and fourth experiments, respectively.

Figure 5 illustrates the good results obtained when the modified ADRCs are required to track a step reference. Both control strategies achieved fast convergence to the reference with a non-oscillatory time response. Besides, the time-delay introduced by the observer dynamics was reduced. The ADRC ID and ADRC ID ADP were tuned with the same parameters: $K_\mathrm{p} = 3.5$, $K_\mathrm{d} = 1.5$, and functions $\ell_1(y-\hat{x}_1) = L_1(y-\hat{x}_1)$, $\ell_2(y-\hat{x}_1) = L_2 f(y-\hat{x}_1, 0.5, \delta)$, $\ell_3(y-\hat{x}_1) = L_3 f(y-\hat{x}_1, 0.25, \delta)$, in (4); with $L_1 = 28.8881$, $L_2 = 278.0063$ and $L_3 = 891.8834$, and $\delta = 1$. When comparing these modified controllers, one can observe that the ADRC ID was more aggressive presenting higher control effort, as can be seen in detail from Figure 5.

In order to highlight the improvement obtained by the proposed modified ADRC in comparison with the pure ADRC strategy, both ADRC ID and ADRC ID ADP were required to track a sinusoidal reference signal, presenting a good performance, and keeping the TRS stable throughout the desired trajectory, as illustrated in Figure 6. Furthermore, due to the smoothness properties of the Algebraic Differentiation Procedure, the ADRC ID ADP presented less control effort than ADRC ID.

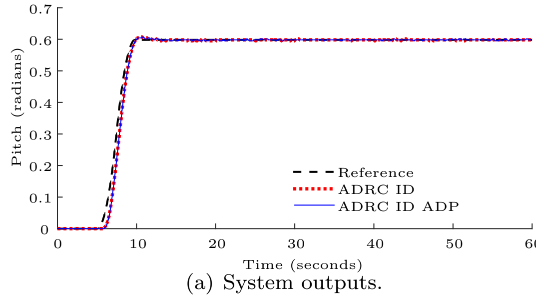

(a) System outputs.

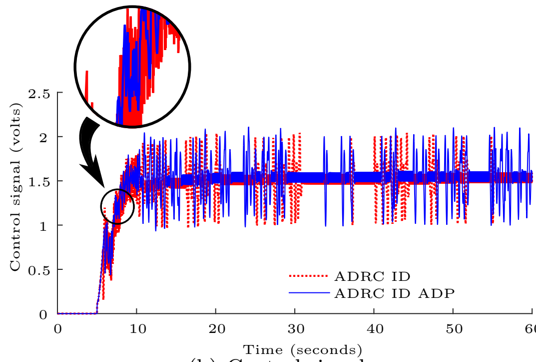

(b) Control signals.

Figure 5: Step response with the modified ADRC strategies.

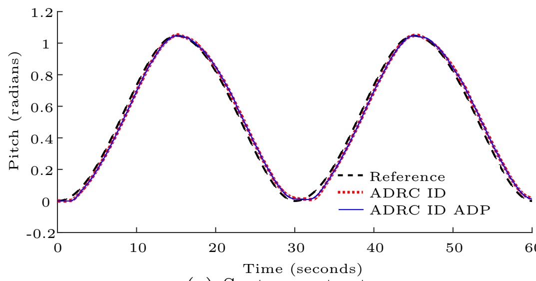

(a) System outputs.

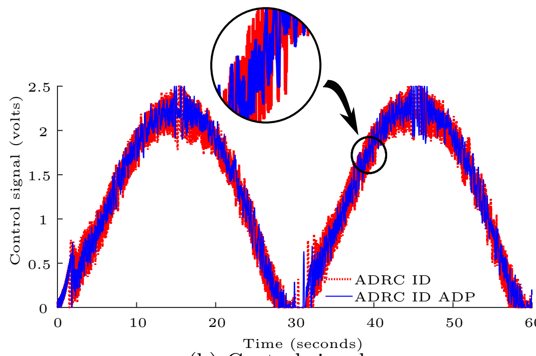

(b) Control signals.

Figure 6: Sinusoidal response with the modified ADRC strategies.

Furthermore, to perform a quantitative analysis of the results obtained with the ADRC ID and ADRC ID ADP when they were submitted to the sinusoidal reference signal, three performance indexes were computed: the Integral of the Absolute Derivative of the control signal

(IADU), given by $IADU = \int_0^\infty \left|\frac{du(t)}{dt}\right| dt$; the Integral of the Squared Error (ISE), given by $ISE = \int_0^\infty e(t)^2 dt$; and the Integral of the Time-weighted Absolute Error (ITAE), computed as $ITAE = \int_0^\infty t\,|e(t)|\,dt$. These results are presented in Table 1. As illustrated in Figure 6, both controllers presented similar tracking response with the computed ISE and ITAE almost the same. However, as highlighted before, the control effort spent by the modified ADRC taking into account the ADP technique is considerably reduced, allowing to achieve better results when the system's output is quantized.

Performance of controllers		
Metrics of the control signal		
Metric	ADRC ID	ADRC ID ADP
IADU	781.5698	271.0811
Error between reference and output system		
Metric	ADRC ID	ADRC ID ADP
ISE	0.0571	0.0574
ITAE	51.7209	51.7709

Table 1: Performance indexes of the modified ADRCs.

Finally, the fifth experiment is realized, to verify the capability of the modified ADRC to deal with disturbances, a step disturbance with amplitude value of 0.5V was applied to the system at $t = 35$s when the TRS was tracking the step reference signal. The results are shown in Figure 7.

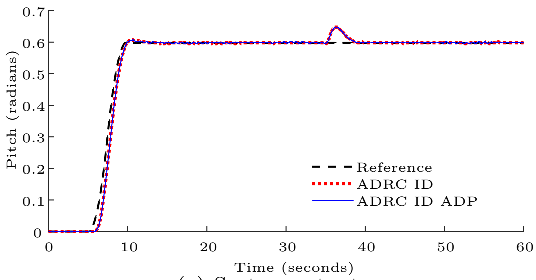

(a) System outputs.

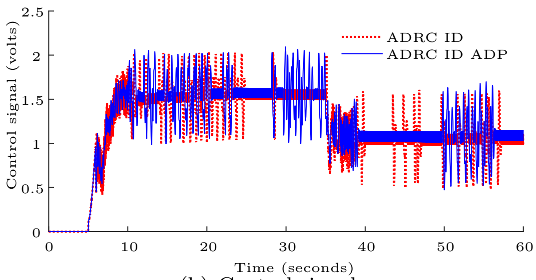

(b) Control signals.

Figure 7: Step response with step disturbance using the modified ADRC strategies.

6 Conclusions

In this work changes to the original ADRC strategy were proposed to deal with quantization in the system's output.

The proposed modified ADRC employs the *Algebraic Differentiation Procedure* and the *Inverse Dynamics*, based on *Robust Exact Differentiator*, techniques to reconstruct the necessary information of the controlled system, allowing to reduce the control effort. This is accomplished by the smoothing of the output signal thanks to the use of the ADP, and by relying on the alleged robustness associated with the ESO in the ADRC strategy.

Experimental results were obtained in order to illustrate the improvement achieved with the proposed strategy. Tests with step and sinusoidal reference signals, and also with step disturbances and uncertain parameters, were carried out. From qualitative and quantitative results it was corroborated the good performance of the ADRC ID ADP with lower control signal power consumption, and small tracking error for sinusoidal references.

7 Acknowledgments

The authors would like to thank the Brazilian research agencies CAPES, CNPq and FAPEMIG for their financial support.

References

Feedback (2006). *Twin Rotor MIMO System Control Experiments 33-949S*, 1 edn, Feedback Instruments Ltd.

Fliess, M. and Join, C. (2013). Model-free control, *International Journal of Control* **86**(12): 2228–2252.

Han, J. (2009). From PID to active disturbance rejection control, *IEEE transactions on Industrial Electronics* **56**(3): 900–906.

Isidori, A. (1989). *Nonlinear Control Systems*, second edn, Springer-Verlag.

Khalil, H. K. (2001). *Nonlinear Systems*, third edn, Prentice Hall.

Levant, A. (1998). Robust exact differentiation via sliding mode technique, *Automatica* **34**(3): 379–384.

Mboup, M., Join, C. and Fliess, M. (2009). Numerical differentiation with annihilators in noisy environment, *Numerical Algorithms* **50**(4): 439–467.

Shtessel, Y., Edwards, C., Fridman, L. and Levant, A. (2014). *Sliding Mode Control and Observation*, Control Engineering, Springer New York.

Slotine, J.-J. and Li, W. (1990). *Applied Nonlinear Control*, Prentice Hall.

Takahashi, R. and Peres, P. (1999). Unknown input observers for uncertain systems: A unifying approach, *European Journal of Control* **5**(2-4): 261–275.

Zehetner, J., Reger, J. and Horn, M. (2007). A derivative estimation toolbox based on algebraic methods – theory and practice, *Proceedings of the IEEE International Conference on Control Applications* (5): 331–336.

Zheng, Q. and Gao, Z. (2016). On active disturbance rejection for systems with input time-delays and unknown dynamics, *2016 American Control Conference (ACC)*, IEEE, pp. 95–100.